

# Parton picture of inelastic collisions at transplanckian energies

O.V. KANCHELI\*

*Institute of Theoretical and Experimental Physics,  
B. Cheremushinskaya 25, 117 259 Moscow, Russia.*

## Abstract

We propose a parton model of inelastic collisions at transplanckian energies  $E \gg G^{-1/2}$ , using the gravitons, whose transverse momenta are cut at the Planck scale, as partons. For this purpose we represent the gravitational shock-wave accompanying the fast particle in terms of such partons and take into account the higher order multiperipheral-like contributions. We argue that the internal part of this shock plane contains the “black” disk of radius  $R(E) \sim E^{1/2}$  filled by such hard partons with the Planck density  $\sim G$ . When two fast particles collide the hard graviton production comes from the region of intersection of their black disks. The corresponding value of inclusive cross-section at the given rapidity and the impact parameter is proportional to the area of this region. The final state with such hard gravitons is unstable relative to the long range gravitational repulsion, and this leads to the creation of the multiperipheral chain of black holes at later stages of the reaction. We discuss various details of this picture including higher order corrections and their connection to a purely classical approach; we also consider briefly possible changes when additional hidden dimensions are present.

## 1 Introduction

The dynamics of particles interaction at transplanckian energies is rather poorly understood up to now, even qualitatively. It is usually believed that at such energies the dominant mechanism of the interaction is a gravitational one, so that its contribution highly overcomes that from other interactions. There is a lot of papers where this problem is considered from a different direction - here we mention only some of them [1] - [9]. The renewal of interest to this topics in last years [10] - [16] is probably connected with the discovery of various brane world like scenarios with TeV-scale gravity [17]. If this will be realized, then gravitation mediated effects can be found already at future accelerator energies.

When two particles with high center-of-mass system (c.m.s.) energy  $\sqrt{s} \gg G^{-1/2} \equiv m_p$  and impact parameter  $B < \sqrt{s} m_p^{-2}$  come close one to another, then the high energy (mass) =  $\sqrt{s}$  is concentrated for a small time in the compact region. For this energy the ‘static’ radius of the horizon of a black hole (BH) with the mass  $\sqrt{s}$  is much larger than the size of the region, where

---

\*e-mail: kancheli@heron.itep.ru

the energy is concentrated. Then, naively, one can expect that in the process of the collision (or even before), an event horizon “surrounding” this region will form, and after this horizon will gradually (at time  $\sim \sqrt{s}/m_p^2$ ) transform to the boundary of a real BH with the mass  $\sim \sqrt{s}$ . But, from the other hand, the colliding particles are highly ultrarelativistic and it is unclear if it is enough time that such a horizon can appear in a causal way.

To refine (or reject) these conclusions number of approaches was developed. The gravitational field of a fast particle with energy  $E$  is concentrated in a shock-wave plane of thickness  $\sim 1/E$  and is usually represented by the Aichelburg-Sexel (AS) metric [18]. The process of a classical collision of two such AS waves is considered in the number of papers. In details it was firstly done in [1] where the transition of one AS wave through another is considered in the geometrical optics approximation. It follows that due to the curving and later focusing of AS planes the curvature singularities can appear. They signal the possible creation of a BH in process. It is also mentioned in [1],[2] that a numerical solution of the Einstein equation for this process also point to a possible appearance of curvature singularities. The other (but in principle the close) method [15] is based on a construction of a maximally large trapped surface in the AS disks collision process and perhaps confirms the same conclusions.

Unfortunately the transition of the one AS disk through another is a very complicated nonlinear process with the unstable behaviour, and it is unclear if one can believe in answers based on the geometrical optics approximation. The other trouble of the simple classical approach is that the curvature in essential parts of AS-disks is too high ( $\gg m_p^2$ ) - and thus all higher order corrections in curvature to the effective Einstein Lagrangian can be of the same order, and this, like in the case of the string interaction, can change the situation drastically - in particular it can soften high curvature effects and freeze them on the  $\sim m_p$  scale. Then all the AS-disk focusing picture [1] can change for  $B < \sqrt{s}/m_p^2$ , because the different degrees of freedom are relevant.

The different approach to transplanckian collisions is the perturbation theory. The diagram with a one graviton exchange leads to the cross-section fast growing with the energy

$$\sigma_{el}(B < B_0) = \int_{k_{\perp min}^2} \frac{d\sigma_{el}}{dk_{\perp}^2} dk_{\perp}^2 \sim G^2 s^2 k_{\perp min}^{-2} \sim B_0^2 \left(\frac{s}{m_p^2}\right)^2, \quad (1)$$

where  $k_{\perp min}^2 = B_0^{-1}$  is the infrared cutoff. The expression (1) hardly violates the unitarity for  $s/m_p^2 \gg 1$  because the allowed maximum of  $\sigma_{el}(B < B_0) \sim B_0^2$ . The eikonalization of the one graviton exchange cures it, and leads [9] to the elastic amplitude

$$A(s, b) = 1 - e^{i\delta}, \quad \delta = 8Gs \ln \frac{B_0}{b}. \quad (2)$$

This amplitude has a simple physical interpretation at the lab.frame of the one of colliding particles, where the phase  $\delta(s, b)$  coincides with the time delay of the target (“test”) particle when it penetrates through the AS shock front at the impact parameter  $b$ .

Other high order corrections to (2) are also considered in the literature - they include the multiperipheral diagrams with gravitons and some generalizations,

similar to that formulated in the gluon (BFKL) case [4, 8]. But no conclusions going far beyond that given by (1) and (2) is reached so far this way. At the same time it is difficult to apply directly such perturbative methods to the region of “small” impact parameters  $b < m_p^{-1}(s/m_p)^{1/4}$ , where, as one can expect, the most interesting effects take place. One needs certain indirect (bypass) way which at the same time preserves the main aspects of the high order perturbation theory, encoded in multiperipheral diagrams and reggeons.

In this paper we speculate how the transplanckian particle collision process can look out in the parton picture. One can hope that by this approach one can take into account the perturbative graviton mechanisms and also include implicitly essential nonperturbative and string effects. The parton picture represents nicely all the main aspects of high energy hadronic interactions, it also shows and “explains” the space-time picture of the process. It can naturally take into account all the regge specifics of the interaction and also that one contained in the dual models. Therefore one can expect that similar methods can be helpful for gravity induced high energy interactions, partially because there is no big difference between graviton and gluon degrees of freedom on the string scale. If partons are chosen successfully, this can give a full qualitative picture of the process and help to find a more accurate way to consider such a phenomenon.

Our “main partons here are the gravitons with the mean virtuality  $\sim m_p$ . We suppose that gravitons with higher virtualities are suppressed in a wave function of the fast particle by some string-like mechanism<sup>1</sup>. And partons with smaller virtualities interact much slowly and lead only to corrections and to infrared effects.

The outline of paper is as follows.

**Section 2.** We consider some classical aspects of the collision relevant to our consideration. We also discuss the popular opinion that the transplanckian gravitational interaction at not large impact parameters can be adequately described in classical terms.

**Section 3.** Here we consider how the wave function of the fast particle can look in terms of such partons-gravitons. We start from the Weizsäcker-Williams (WW) like partons, decomposing the classical AS field and then try to refine the model by the inclusion of graviton interactions and cascading. The hard parton-graviton density is large in a transverse disk with the radius  $\sim m_p^{-1}\sqrt{E}$ , and we suppose that inside of such a disk the 2D parton density is saturated at the Planck scale.

**Section 4.** We consider the collision of two such disks and study main inelastic processes. The resulting final state depends essentially on the impact parameter of the collision and consists from layers multiperipherally distributed in rapidity and filled with gravitons. In every such layer the relative velocities of gravitons are locally thermalized, with relative energies  $\sim m_p$ . The process of the creation of this final state takes a long time  $\sim m_p^{-2}\sqrt{s}$ , and the order in which these layers are created is system dependent, like in the usual multiperipheral picture.

**Section 5.** Then we consider the future time evolution of such a multiparticle state, created in a parton disks collision. The classical instabilities, due to a long range attraction between particles with not large relative velocities, can take place and lead to the creation of the “multiperipheral” chain of BH from

---

<sup>1</sup>The string-bit model [20, 21] is in some respects similar to the hard parton constructions we used above, but it starts directly from a fast string state

particles collapsing in every layer.

**Section 6.** In conclusion we discuss some questions related to this picture.

## 2 Some classical aspects of collision

The gravitational field of a fast particle with the mass  $m \ll m_p = G^{-1/2}$  can be found by boosting of the static Newton field. For a very high energy  $E \gg m_p$  it gives approximately the same as the boosted Schwarzschild field

$$g_{\mu\nu} - g_{\mu\nu}^{(0)} \simeq \frac{2GP_\mu P_\nu}{m} \frac{1}{\sqrt{x_\perp^2 + \gamma^2(z - \beta t)^2}} \quad , \quad (3)$$

where  $g_{\mu\nu}^{(0)}$  is the Minkowski metric,  $P_\mu$  - fast particle 4-momenta,  $\gamma = E/m$ ,  $\beta = p/E$ . By going to the limit  $\beta \rightarrow 1$  and making an additional singular in  $t, z$  coordinate transformation, one usually represents this metric in the AS form

$$ds^2 = dx^+ dx^- + 4GE \ln x_\perp^2 \delta(x^-) (dx^-)^2 - (dx_\perp)^2 \quad , \quad (4)$$

where  $x^+ \equiv v = t + z$ ,  $x^- \equiv u = t - z$ ,  $x_\perp$  are the light-cone coordinates. Another method to become the AS metric which can be simply applied also to a distributed light-like matter ( $\sim$  partons), is based on the old observation that for a general right-moved plane metric

$$ds^2 = dx^+ dx^- + f(x^-, x_\perp) (dx^-)^2 - (dx_\perp)^2 \quad (5)$$

Einstein equations reduce to a simple Poisson form

$$R_{--} = \partial_\perp^2 f(x^-, x_\perp) = G T_{--}(x^-, x_\perp) \quad (6)$$

For a bunch of massless particles with energies  $\varepsilon_n$  and coordinates  $(z_n, x_{n\perp})$ , moving along the  $z$  axis, with the energy-momentum tensor

$$T_{--}(u, x_\perp) = \sum_n \varepsilon_n \delta^2(x_\perp - x_{n\perp}) \delta(u - z_n) \quad . \quad (7)$$

it follows, due to linearity of (6), that

$$f = 4GE \sum_n \left( \frac{\varepsilon_n}{E} \right) \delta(x^- - z_n) \ln(x_\perp - x_{n\perp})^2 \quad . \quad (8)$$

For  $n = 1$  this reduces to the AS metric (4). For one point-like particle the curvature fields are concentrated in a plane shock-front  $\delta(x^-)$ , like the electric and the magnetic fields for a fast Coulomb particle, where the same structure  $\delta(x^-) \ln x_\perp^2$  enters the expression for potentials <sup>2</sup>. For the metric of type (5) the only nonzero components of the curvature tensor are

$$R_{-\perp-\perp} = -\partial_\perp \partial_\perp f(x^-, x_\perp) \sim \delta(x^-) x_\perp x_\perp / x_\perp^4 \quad , \quad (9)$$

where the last expression is for a point-like particle. The curvature tensor for (3) has approximately the same structure as (9), but is evidently smeared in  $x^-$

<sup>2</sup>The often mentioned analogy of the AS type metric with shock waves is very superficial. In usual shock waves the energy is concentrated not in the front discontinuity but in a long layer of the gas moving behind the front.

on  $mx_{\perp}/E$  and, what is in a certain sense essential, its Weyl part belongs to a different canonical type.

In connection with the previous is also such a property of the AS metric (4), and also of the more general one (5), that the corresponding symmetrical energy-momentum pseudotensor  $\theta_{\mu\nu}^{(LL)}$  vanishes - so that it is hard to define in a consistent way the energy contained in AS type field <sup>3</sup>. But for the boosted Schwarzschild metric (3) the  $\theta_{\mu\nu}^{(LL)}$  is nonzero - it has only one large component

$$\theta_{--}^{(LL)} \sim \frac{G\gamma^2 m^2}{(x_{\perp}^2 + (\gamma x^-)^2)^2}, \quad (10)$$

as is normal for an ultrarelativistic object. The energy flow in this case is

$$\varepsilon(x_{\perp}) \simeq \int_{-\infty}^{\infty} dx^- \theta_{--}^{(LL)} \simeq \frac{1}{x_{\perp}^3} \left(\frac{m}{m_p}\right) \left(\frac{E}{m_p}\right),$$

and the quantity

$$\varepsilon \simeq \int_{1/m}^{\infty} d^2 x_{\perp} \varepsilon(x_{\perp}) \sim \left(\frac{m}{m_p}\right)^2 E$$

gives the energy in the coherent gravitational field of fast particles.

The massless test particles colliding with the AS disk on the distance  $x_{\perp}$  from the center will be captured (trapped) by a disk for time  $= 8GE \ln(L/x_{\perp})$ , and during this time transported backward in  $z$  to the distance  $8GE \ln L/x_{\perp}$  and then released from opposite side of the AS disk (See Fig. 1). After that particles

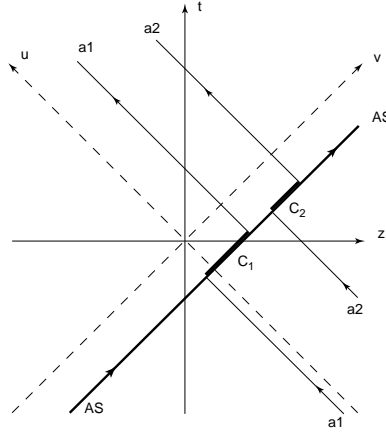


**Fig.1 :** Trajectories of “test” particles  $a_1$  and  $a_2$  colliding with the AS disk accompanying a fast transplanckian particle. On the sections  $C_1$  and  $C_2$  the particles are “transported” by the AS disk.

continue their motion with the same momenta as before the collision <sup>4</sup>.

<sup>3</sup>This takes place not only for a Landau-Lifshitz form of  $\theta_{\mu\nu}^{(LL)}$ . The other popular forms of  $\theta_{\mu\nu}$ , for example the canonical one, also give zero. This zero is the result of the change of the canonical Weyl tensor type in the AS case - which by itself follows after the singular coordinate transformation made while going from (3) to (4).

<sup>4</sup>Such a behavior is a simple reflection of that phenomena that in the gravitational field of

Trajectories of these test particles look discontinuous (if we “forget about sections  $C_1$  and  $C_2$  on Fig.1, where particles simply move backward glued to the AS plane). One can perform the specific coordinate transformation [1], singular in the AS plane, so to make the test particles trajectories, crossing the AS plane, continuous. Making it one cuts out a region of the space-time around the AS plane (of  $1/E$  thickness), after that shifting and gluing together the distant planes. But this procedure looks very strange and risky for a nonsingular metric (3), for which the test particle trajectories are continuous.

The classical collision of two AS disks is considered in the number of works but no exact solution showing how they move one through another was found. The most detailed analysis of this process was first given in the paper of D’Eath [1] (See also [2] and papers cited there). One can mention three main approaches to this problem. One is based on a numerical solution of Einstein equation, another on the geometrical optics approximation, and the third on the analysis of the possible appearance of trapped surfaces during the process of the two AS disks collision.

In the geometrical optics approximation one of the AS surface is treated as a system of many infinitesimal test particles (directrix) which cross the another AD disk and do not disturb them during the traverse period. The same is symmetrically done with another AS-disk. Because the time-delay depends on  $x_\perp$ , during such a transition of the AS fronts one through another, they curve. At later times these curved AS disks focus on caustic surfaces, where their curvature becomes very big, and this signals about the creation of some BH like objects, possibly surrounded by horizons. As mentioned in [2], the consideration of the same problem by means of a numerical solution of Einstein equations gives the reminding picture.

Another approach is based on a search of possible trapped surfaces shortly before the AS-disk’s collide [1, 15, 16]. If such a surfaces exist, one usually predicts that a black holes will be created in process of the collision and even estimates their mass and the corresponding cross-section for the inelastic interaction. Such a consideration is usually done in specially transformed coordinates, singular with respect to the “normal” one and chosen in such a way to make the test particles trajectories “continuous”, when they cross the AS surface. This is a risky procedure because some effects can arise due to the singular structure of AS planes and the real answer can depend on that what takes place when two singular AS planes go one through another in the period of their collision, where we in fact do not know the metric.

At the same time one can try to consider this in “usual” nontransformed coordinates. The picture is illustrated by Fig.2 where the configuration of two disks is shown for some time before the collision. The region  $\Gamma$  is defined in such a way that the massless test particle can not escape from this region before the AS disks coincide. The space between disks is flat. But when a particle will try to escape from the region  $\Gamma$  it will collide with one of the disks and will be absorbed (glued) and transported with it towards another AS disk. The

---

a “standing” particle time is delayed. So moving in this field massless particles are slightly slow down (remain behind in  $z$ ) near the mass on time  $\delta t \simeq 4Gm \ln(L/x_\perp)$ , where  $L \gg x_\perp$  is the full distance in  $z$  that particles traveled. As a result they remain behind in  $z$  from the similar trajectories with larger  $x_\perp$ . If we boost this time delay by gamma-factor  $\sim E/m$  we come to the space-time delay  $4GE \ln(L/x_\perp)$ , and this corresponds to the picture of the motion of the test particle captured by the AS front.

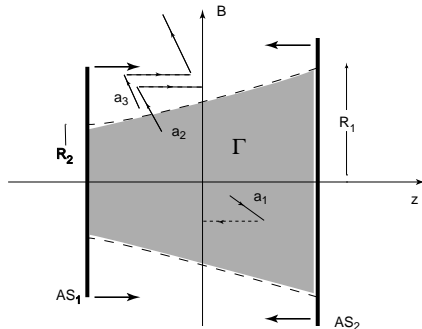


**Fig.2 :** Particles from  $\Gamma$  - the filled region between approaching one to another AS disks can not escape to infinity. They collide with disks  $AS_1$  or  $AS_2$  and after that are transported to the plane  $z = 0$  where two disks coincide(merge), before particle come out from other side of disks. Particles  $a_1$  and  $a_2$  shown on Fig. are trapped and particle  $a_3$  have time to cross the  $AS_1$  disk and escape. This type condition in fact fully defines the shape of region  $\Gamma$  for all  $B$  and  $y$ .

longitudinal and the transverse size of  $\Gamma$  can be defined from the condition that the particle glued to one of  $AS_i$  disks will not be released (from another side of the disk) before disks collide. The region  $\Gamma$  is maximal in c.m.s. and for  $B = 0$ , when it is cylinder with the radius  $x_{\perp}$  and the height  $Z = 2x_{\perp} = 8GE$ . In the frame, where particles have energies  $E_1, E_2$  but again  $B = 0$ , the region  $\Gamma$  is a truncated cone with foundations  $R_i = 4GE_i$  and  $Z = 4G(E_1 + E_2)$ . For  $B \neq 0$  the shape of  $\Gamma$  is deformed (see [16]).

But how can one conclude only from the existence of a region  $\Gamma$  with such a properties that anything singular happens in the future evolution of the AS disk system? Evidently that this future depends only on that what takes place on a complicated nonlinear stage when two AS disks (smeared in  $z$  by  $\sim 1/E_i$ ) coincide. And the existence of the empty region  $\Gamma$  nothing changes in this respect. When regarded from such a position, the trapped surface found in coordinates with continuous trajectories can be the artifact of using the singular coordinates. Another risky moment of using the trapped surfaces for the prediction of the future system evolution is that these trapped surfaces are isolated from the “rest world” by the the AS shock fronts where the curvature is singular (or partially coincide with the  $AS_i$  planes). And the last moment. If for colliding particles we use the regular metric (3), instead of the AS, then the previous consideration of  $\Gamma$  (like in Fig.2) remains unchanged. But if some trapped surfaces exist in this case is rather unclear now and needs an additional investigation. It is possible that the classical “singular” methods as used in [1, 2, 16] lead to more or less adequate answer for the BH production, but the physics of this is not evident.

At the end of this section two additional remarks

- The whole picture of the AS disks collision should be longitudinally boost covariant, when we change the energies of colliding particles  $E_1 \rightarrow E_1\xi$ ,  $E_2 \rightarrow E_2/\xi$  leaving  $s \simeq 2E_1E_2$  and the impact parameter  $B$  invariant. By this transformation we can always select a frame in such a way that

it is close to the “laboratory” frame, when one of the energies is very big  $E_1 \gg m_p$  and the another is “arbitrary” small  $E_2 \ll m_p$ . Moreover, because the mass of the particles is “in our hands” we can make the energy  $E_2$  so small that it can be considered as a “test particle” with the respect to the particle  $E_1$ . In such a system the “trapping” region  $\Gamma$  disappears and all the space-time before the  $AS_1$  disk corresponds to the region of the intersection of two disks in c.m.s. ( $z = 0$  in Fig.2). Now we have only one AS disk and an additional light-like test particles can move to infinity without any intersection with the  $AS_1$  plane. All this means that if we hope that some classical curvature singularities must necessary appear in such a collision (remember that  $s \gg m_p^2$ ), then, in this system, they must originate from an instability of the individual AS disk with the respect to a small disturbances.

- The curvature in the AS shock front is high - for the transplanckian case it is much larger than the critical one - for some components of the curvature tensor  $|R_{\mu\nu\lambda\sigma}| \gg m_p^2$ . Therefore in the effective gravitational Lagrangian the higher order terms in  $R_{\mu\nu\lambda\sigma}$  can be of the same order of the magnitude (or even bigger) than the standard  $R$  term. Such terms can be induced by the quantum fluctuations or “come from strings”. For the metric of type (5) this will correspond to additional terms at the left hand side of Eq.(6):

$$\partial_{\perp}^2 f(x^-, x_{\perp}) + c_2 m_p^{-2} (\partial_{\perp}^2 f(x^-, x_{\perp}))^2 + \dots = G T_{--} \quad (11)$$

These terms can radically change the structure of AS solution for  $E \gg m_p$ , smoothing the entering (8) singularities<sup>5</sup>. Also, depending from signs and relative values of nonlinear terms in (11), this can lead, for example, to a saturation of values of  $f$  in the internal parts of AS disk, where  $f$  in the linear case can be arbitrary big.

### 3 Parton structure of fast particle with $E \gg m_p$

To understand the AS shock fronts interaction, when the classical picture is unreliable, we introduce the “microscopic” model of the AS disk in terms of parton degrees of freedom. There is a number of possibilities for a choice of constituents (partons) Various degrees of freedom or there combinations can be used as partons but it is very difficult to choice between them the most adequate one. It is possible the string coordinates (or string bit’s [20]) are the most appropriate ones. But the dynamics at the high string density is also unclear - it is possible here again we come to a particle-like media. We use the transverse gravitons as partons, and regulate their spectra at  $k_{\perp} \geq m_p$  in a way suggested by “strings”. Going to Fourier components of the metric

$$\sum_{\lambda} a^{\lambda}(k) \epsilon_{\mu\nu}^{\lambda} = \omega \int d^3x e^{ikx} ( g_{\mu\nu}(x) - g_{\mu\nu}^{(0)}(x) ), \quad (12)$$

where  $\epsilon_{\mu\nu}^{(\lambda)}$  -gravitons polarization tensors,  $\omega = \sqrt{k_z^2 + k_{\perp}^2}$ , and substituting into the right hand side of (12) the AS metric components from (4) or from (3)

<sup>5</sup>For one light particle state one can always, by moving to a rest frame, make the contribution of additional terms in (11) small. But for colliding transplanck particles these terms can be very essential, especially in a AS-disk’s intersection region.



we find:

$$\sum_{\lambda} a^{\lambda}(k) \epsilon_{--}^{(\lambda)} = \frac{E}{m_p} \omega \frac{1}{k_{\perp}^2} . \quad (13)$$

From the transversality condition  $k^{\mu} \epsilon_{\mu\nu}^{(\lambda)} = 0$  in the gauge  $\epsilon_{+\mu}^{(\lambda)} = 0$  we have the following relation between longitudinal and transverse projections of polarization tensor :

$$\epsilon_{--}^{(\lambda)} = \epsilon_{\perp\perp}^{(\lambda)} \frac{(k^+)^2}{k_{\perp}^2} . \quad (14)$$

With the fields normalization used in (12), the full parton (graviton) number in a fast particle field is given by :

$$N = \int d^3k n(k) = \int \frac{d^3k}{\omega} \sum_{\lambda} a^{\lambda}(k) a^{+\lambda}(k) . \quad (15)$$

Then, substituting (13) and (14) in (15), we can extract the transverse graviton density in the AS disk :

$$\begin{aligned} dn^{\perp}(E, \omega, k_{\perp}) &\sim \frac{(a^{\lambda})^2}{\omega} d\omega d^2k_{\perp} \sim \\ &\sim \left(\frac{E}{m_p}\right)^2 \frac{\omega}{(k^+)^4} dk_z dk_{\perp}^2 \sim \left(\frac{E}{m_p}\right)^2 \frac{d\omega}{\omega^3} d^2k_{\perp} , \end{aligned} \quad (16)$$

These spectra differs crucially from the QED vector parton spectra<sup>6</sup>, by the  $\omega$  and  $k_{\perp}$  dependence and by the overall growth of the parton density  $\sim E^2$ .

In a ‘‘full’’ theory one can expect that the spectra (16) are essentially suppressed at  $k_{\perp} > m_p$  due to various nonlocal ‘string’ effects. Here we simply suppose that they are cut at  $k_{\perp} \geq \kappa \sim m_p$ . Then the following integrated over  $k_{\perp}$  spectra

$$dn^{\perp}(\omega) = d\omega \cdot \int_0^{\min(\omega, \kappa)} d^2k_{\perp} n^{\perp}(\omega, k_{\perp}) \sim \left(\frac{E}{m_p}\right)^2 \frac{\kappa^2}{\omega(\omega^2 + \kappa^2)} d\omega \quad (17)$$

can be approximately used for all  $\omega$ .

Now let us discuss how essential are the higher order corrections to these primary parton spectra. The main higher order diagrams at high energies, which ‘‘follow’’ the WW contribution - are the multiperipheral ones. In terms of partons they correspond to a parton cascading which increases with  $E$  the full number of low energy partons, and as a result the cross-sections<sup>7</sup>. Such graviton ladder corrections for a scattering amplitude are considered in a number of papers [3] in the pure gravity, supergravity and also for ‘‘multiperipheral’’ string amplitudes [8]. We will not review here these calculation - for our qualitative consideration we only mention some aspects essential for us. Firstly we suppose that such ladders are supplemented by some vertex factors  $\Gamma(k_{i\perp}/m_p^2)$  that

<sup>6</sup>The parton spectra (16) can be found also from the WW like factorization of one graviton exchange diagram as is usually done for photons in QED books. It is instructive to compare the expression (16) with the general form of WW spectra for the spin J field

$$dn^{\perp} \sim g_J^2 \left(\frac{k_{\perp} E}{\omega}\right)^{2J} \left(\frac{\omega d\omega}{E^2}\right) \frac{d^2k_{\perp}}{k_{\perp}^4} = g_J^2 \frac{dx}{x^{2J-1}} \frac{d^2k_{\perp}}{k_{\perp}^{2(2-J)}} ,$$

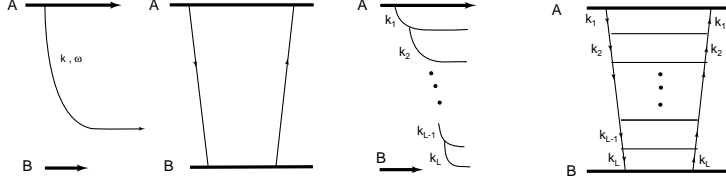


**Fig.3 :** The fast particle A with its parton cloud interacts with the target B ; (a) and (b) represent the WW amplitude and one cell ladder corresponding to a WW cross-section ; diagrams (c) and (d) represent the graviton cascading and the ladder amplitude corresponding to a cross-section of the interaction with the target

smoothly cuts high virtual transverse momenta  $k_{i\perp} > m_p$  on exchanged lines (see Fig.3). Then for integrations over  $k_{i\perp}$  in all cells of the ladder the mean contribution comes from the region near this upper bound  $k_{i\perp} \sim m_p$ .

The averaged picture of the “ladder”-cascading process in parton terms can be represented as a chain of  $L$  step convolutions of the “primary” WW spectra  $n^\perp(\omega_i, \omega_{i+1}, k_\perp)$  given by (16). This gives:

$$\begin{aligned} & \int d\omega_1 d^2 k_1 n^\perp(E, \omega_1, k_1) \int d\omega_2 d^2 k_2 n^\perp(\omega_1, \omega_2, k_2) \dots \\ & \dots \int d\omega_{L-1} d^2 k_{L-1} n^\perp(\omega_{L-1}, \omega_L, k_L) \sim \quad (18) \\ & \sim \frac{\Delta^L}{(L-1)!} \left(\frac{E}{m_p}\right)^2 \frac{1}{\omega_L^3} \ln^{L-1}\left(\frac{E}{\omega_L}\right) , \end{aligned}$$

where

$$\Delta = m_p^{-2} \int d^2 k_\perp \Gamma^2\left(\frac{k_\perp^2}{m_p^2}\right) ,$$

and where, as have mentioned above, we included the effective graviton emission vertexes  $\Gamma$  in the density  $n^\perp$  to take into account nonlocal effects responsible for the cutoff of high  $k_\perp$ . Summing over the number of cascade steps  $L$  we come to the “reggeized” graviton-parton spectra

$$dn^\perp(E, \omega, k_\perp) = \left(\frac{E}{m_p}\right)^2 \left(\frac{E}{\omega}\right)^\Delta \frac{d\omega}{\omega^3} d^2 k_\perp . \quad (19)$$

where  $g_j$  is the corresponding coupling constant :  $g_1 \leftrightarrow e_{qed}$ ,  $g_2 \leftrightarrow \sqrt{G}$ , ... and  $x$  - Feynman scaling fraction  $\omega/E$ .

<sup>7</sup> The parton cascading gives the shift of the reggeon intercept  $\alpha(0)$  from their bare values. This corresponds to an additional growth of the parton density by the factor  $\sim (E/\omega)^\Delta$ , when we go to smaller parton energies  $\omega$ . The average interval in rapidity between the parton splitting (ladder rungs) is  $\sim 1/\Delta$ . In the BFKL [23] case (vector partons) the shift of the pomeron intercept  $\alpha(0)$  from their bare value is  $\Delta \sim g_{QCD}^2$ , but the gluon intercept probably does not shifts because of the gauge nature of gluon. The gravitons intercept probably also do not change, by the same reason. But the intercept of the bare 2G trajectory ( $= 3$ ) corresponding to (16) can shift, if nothing prevents.

Such corrected parton spectra are even more concentrated<sup>8</sup> at low  $\omega$  than the primary WW spectra (16), and the value of  $\Delta$  gives shift of bare WW intercept ( $=3$ ).

The other important higher order corrections, besides the parton cascading and various rescatterings (like eikonalization), correspond to the parton recombination which become essential when the parton density is high, and this process can lead to the parton density saturation.

Due to the masslessness of gravitons there is also the ‘infrared’ contribution, coming from small  $k_{i\perp} \rightarrow 0$ . In the first WW approximation this corresponds to the large impact parameter elastic scattering. If some cells, in hard ladder, contain small  $k_{i\perp} \rightarrow 0$  than in the impact parameter space this will correspond to big  $\delta b \sim k_{i\perp}^{-1}$  steps, “transporting” part of the hard ladder far in  $b$ . In terms of t-channel regge amplitudes this corresponds to the  $k_{\perp}^2 \ln k_{\perp}^2$  type singularities, coming from such infrared cells.

Firstly we illustrate this in terms of the parton cascading. Suppose that the first step (cell) is infrared and consider it. Then the parton distribution (16) at large transverse distances  $x_{\perp} \gg m_p^{-1}$  can be represented in the form

$$\frac{\partial n}{\partial \omega \partial^2 x_{\perp} \partial^2 x_{\perp}} \sim \left(\frac{E}{m_p}\right)^2 \frac{1}{\omega^3} \tilde{\delta}\left(x_{\perp}^2 - \frac{1}{k_{\perp}^2}\right) \sim \left(\frac{E}{m_p}\right)^2 \frac{1}{\omega^3} \frac{1}{x_{\perp}^4} \tilde{\delta}\left(k_{\perp}^2 - \frac{1}{x_{\perp}^2}\right), \quad (20)$$

where  $\tilde{\delta}$  is narrow  $\delta$ -like function, having width of peak  $\sim 1$ . Integrating (20) over  $k_{\perp}$  we become the distribution of these partons in the transverse (impact parameter) plane  $x_{\perp}$

$$\frac{\partial^3 n}{\partial \omega \partial^2 x_{\perp}} \sim \left(\frac{E}{m_p}\right)^2 \frac{1}{\omega^3} \frac{1}{x_{\perp}^4}, \quad (21)$$

which we use for  $x_{\perp} \gg m_p^{-1}$ . All this corresponds simply to the approximation  $\partial n / \partial x_{\perp} \sim \partial n / \partial k_{\perp}^{-1}$ . But if we insert two or more infrared cells to the cascade chain (18), we come to a much smaller contribution at large  $b$ . Indeed, in this case we have the convolution of two distributions (21) containing integrals

$$\int_{|x_{\perp} - b_i| > m_p^{-1}} d^2 x_{\perp} / (b_1 - x_{\perp})^4 (x_{\perp} - b_2)^4 \sim m_p / (b_1 - b_2)^4$$

which for  $(b_1 - b_2)^2 \gg m_p^{-2}$  gets the main contribution near the integration ends, where one of these cells enters in the hard regime. The distribution (21) at  $x_{\perp} \gg m_p^{-1}$  refers to soft gravitons, but inserted in the cascading chain these partons are the sources for the next hard chain sections. Then the simple generalization of (18) and (21) gives the  $x_{\perp}$  distribution

$$\frac{\partial^3 n}{\partial \omega \partial^2 x_{\perp}} \sim \left(\frac{E}{m_p}\right)^2 \left(\frac{E}{\omega}\right)^{\Delta} \frac{1}{\omega^3} \frac{1}{x_{\perp}^4}, \quad \frac{\partial n}{\partial x_{\perp}^2} \sim \left(\frac{E}{m_p}\right)^{2+\Delta} \frac{m_p^2}{(m_p x_{\perp})^4} \quad (22)$$

<sup>8</sup>The value of  $\Delta$  depends strongly on the behaviour of the nonlocal factor  $\Gamma$ . In the perturbative string approach the value of  $\Delta$  can be small  $\sim g_s^2$ , where  $g_s$  is the string constant, if the “cutoff” in  $k_{\perp}$  is on the string scale and not on the Planck scale, and the higher string modes entering loops will not compensate this. But if we include in cascading all other (not only ladder) diagrams, the value of  $\Delta$  can be turn out to zero. This follows from the momentum sum rules for the parton distribution  $n^{\perp}$ . The additional arguments in favor of the condition for a final  $\Delta = 0$  are given in the end of section 4

for hard partons with  $\langle k_{\perp}^2 \rangle \sim m_p^2$  and  $x_{\perp} \gg m_p^{-1}$ .

Now consider the interaction of a fast particle, with parton spectrum (19), with a pointlike target. The cross-section is

$$\sigma_{in} = \int d\omega d^2k_{\perp} n(E, \omega, k_{\perp}) \hat{\sigma}(\omega, k_{\perp}) \sim s^{2+\Delta}, \quad (23)$$

where  $\hat{\sigma}$  is the parton cross-section on a local target. Such a behaviour corresponds to a regge pole with the positive signature in a vacuum channel and with the intercept

$$\alpha(0) = 3 + \Delta. \quad (24)$$

This regge pole can be considered as an analog of the pomeron for the gravitational interaction<sup>9</sup> (later, for abbreviation, we will call this reggeon 2G). The same cross-section (23), written in the impact parameter space, looks like

$$\sigma_{in}(s, b) \sim \left(\frac{s}{m_p^2}\right)^{2+\Delta} \frac{1}{(bm_p)^4} \quad (25)$$

The singularities of (25) in  $t = -q_{\perp}^2$  can be represented by the following expression

$$e^{-\alpha' q_{\perp}^2 \ln s} \left( a_0 + a_1 q_{\perp}^2 \ln \frac{1}{q_{\perp}^2} + a_2 (q_{\perp}^2 \ln \frac{1}{q_{\perp}^2})^2 + \dots \right), \quad (26)$$

giving the main factors for an associated t-channel amplitude, where terms with coefficients  $a_i$  correspond to a contribution with  $i$  infrared cells (loops) in the parton cascade. These terms lead to the  $b \gg m_p^{-1}$  behavior generalizing (25):

$$\begin{aligned} \sigma_{in}(s, b) \sim & \left(\frac{s}{m_p^2}\right)^{2+\Delta} \left( \frac{a_0}{\ln s} \exp\left(\frac{-b^2}{4\alpha' \ln s}\right) + \right. \\ & \left. + \frac{a_1}{(bm_p)^4} + \frac{\tilde{a}_2 \ln b}{(bm_p)^6} + \dots \right) \end{aligned} \quad (27)$$

We see that at large  $b$  only terms with one infrared cell are essential. And thus terms in (26), singular in  $q_{\perp}$ , can be included in vertices connected with the exchange by the 2G reggeon, with the intercept (24). On the contrary, in massive theories like the QCD, only a first term in (27) is present at all  $b$  (this is a standard regge pole contribution). As a result this leads to a fast cutoff of  $\sigma_{in}(s, b)$  in  $b$  and, after the unitarization, to the Froissart-like behavior  $\sim \ln^2 s$  of cross-sections.

The cross-sections  $\sigma_{in}(s, b)$  grow fast with  $E$  and for some  $E$  exceed the maximal value = 1 allowed by unitarity, when all incoming particles flux at given  $b$  is absorbed. This means that the parton screening becomes essential. The simplest way to take screening corrections into account is to use the eikonalization :

$$\sigma_{in}(s, b) = 1 - |S(s, b)|^2 = 1 - \exp(-2\sigma_{in}^0(s, b)), \quad (28)$$

<sup>9</sup>It seems that there is no such state between the perturbative states in known sectors of string theories containing the gravity. But it can be a composite state seen only at the strong coupling. It is possible as well that this state is masked by the singularity corresponding directly to a black disk (some brane-like object ?).

where  $\sigma_{in}^0$  is given by (27). The  $S$ -matrix, entering (28), contains, among others, a “black disk”, where the parton density exceeds the “critical” one  $\sim m_p^{-2}$ . This is in the internal part of the AS disk where

$$x_\perp^2 < R_\perp^2(E) = m_p^{-2} \left( \frac{E}{m_p} \right)^{1+\Delta/2} \quad (29)$$

Outside this ‘black’ part where  $x_\perp > R_\perp(E)$  the density decreases as :

$$\frac{\partial n}{\partial x_\perp^2} = m_p^2 \left( \frac{R_\perp(E)}{x_\perp} \right)^4 \quad (30)$$

For  $b < R_\perp^2(E)$  the screening of partons in a process of the interaction is essential and the expression (28) takes it into account. But, at the same time, it corresponds to that all these partons are nevertheless present in the incoming state. And therefore, there 2 D density (in parton state) anyway highly exceeds the Planck density  $m_p^{-2}$ . But then the mean transverse momenta of these partons, due to their strong interactions, also can be much greater than the Planck scale. And this is inconsistent with our previous assumption that all  $k_\perp$ , much higher than  $m_p$ , are cut. Therefore we also suppose that the parton density saturates at the Planck scale and does not increase with  $E$  in an internal parts of the AS disk, where  $x_\perp < R_\perp(E)$ . The dynamical mechanism responsible for such a density stabilization (saturation) can be probably represented as a parton recombination, like that in the vector (BFKL) case <sup>10</sup>.

The full  $S$ -matrix corresponding to (28)

$$S(y, b) = e^{i\delta_R(y, b) - \delta_I(y, b)} \quad , \quad \delta_I(y, b) \sim \sigma_{in}^0(s, b) + \dots \quad (31)$$

contains also a real part of the phase  $\delta_R(y, b)$ , which for very large  $b$  coincides with the “classical” AS phase

$$\delta_R(y, b) \sim \left( \frac{s}{m_p^2} \right) \ln \frac{B_0}{b}$$

and is responsible for a large  $b$  elastic scattering. This  $S$ -matrix gives the hard inelastic cross-section

$$\sigma_{in} = \int d^2b (1 - e^{-\delta_I(b, y)}) \simeq \pi R_\perp^2(y) \sim m_p^{-2} \left( \frac{s}{m_p^2} \right) \quad , \quad (32)$$

corresponding to the same structure of a black absorbing disk with the radius  $R_\perp(y) \sim \sqrt{s}/m_p^2$  as given by the expression (29). Such a disk remains a Froissart black disk and the method by which it is often introduced from the eikonalization

---

<sup>10</sup> There are signs that the string system undergoes some phase transition at Hagedorn temperatures to some new phase, and there are arguments [19] that this phase is not a string like. For the high string densities the situation is probably the same. And more, there exists a popular opinion formulated in various forms that virtual (parton) string states with the transplanckian density of degrees of freedom  $\gg m_p^{-D}$  (even local) are inaccessible, because their contribution is strongly damped (possibly exponentially in density) in the wave function. Despite the fact that such a reduction of high density states can be encoded in very general constructions, like holographic principle or M-theory, the concrete mechanism doing this in all cases can be simply a more fast recombination of additional degrees of freedom than their creation, when some critical density is reached.

of supercritical pomeron exchange. The difference is the behaviour of the black disk radius with the energy :  $R \sim m^{-1} \ln(s/m^2)$  for the Froissart case (for massive theories), and  $R \sim m_p^{-2} \sqrt{s}$  for the massless gravitation <sup>11</sup>.

We considered above only partons with  $\omega \sim m_p$ , where the majority of hard partons are concentrated. We can extend this to partons with different  $\omega$  and find their distributions. Simple generalization of it gives the parton spectra at arbitrary  $\omega$  and  $x_\perp$

$$dn = \hat{n}(E, \omega, x_\perp) (m_p^2 d^2 x_\perp) \frac{d\omega}{\omega}, \quad \hat{n} = \left(\frac{E}{\omega}\right)^{2+\Delta} \frac{1}{(x_\perp m_p)^4}, \quad (33)$$

where the density  $\hat{n}$  is dimensionless and boost invariant. This distribution takes an even more simple form if we go to rapidities  $Y = \ln E/m_p$ ,  $y = \ln \omega/m_p$  and to  $\zeta = \ln(x_\perp m_p)^2$  :

$$dn = e^{(2+\Delta)(Y-y)-\zeta} dy d\zeta \quad (34)$$

From the condition  $\hat{n} \sim 1$  we find the black disk radius for various  $\omega$  :

$$R_\perp^2(E, \omega) = m_p^{-2} \left(\frac{E}{\omega}\right)^{1+\Delta/2} \quad (35)$$

Thus the saturated part of a hard parton configuration in  $(\zeta, y)$  space consists from a “cone”, with the boundary  $\zeta < (2 + \Delta)(Y - y)$  (this corresponds to  $x_\perp < R_\perp^2(E, \omega)$ ), filled with the density  $\sim 1$  ( $\sim m_p^{-3}$  in units  $x_\perp$ ). This cone is surrounded by a more “diffuse” soft ( $\omega \ll m_p$ ) cloud, where the parton distribution is given directly by (34).

For  $\omega \ll m_p$  the parton density  $\hat{n}$  in this soft tail can be very large  $\hat{n} \gg 1$ . The mean transverse localization of these partons is  $\delta x_\perp \sim 1/\omega$ . Comparing it with the size of the region  $R_\perp(E, \omega)$  where  $\hat{n} > 1$  we can find the soft critical radius and the parton frequency

$$\tilde{R}(E) \sim m_p^{-1} \left(\frac{E}{m_p}\right)^{1+2\Delta/(2-\Delta)}, \quad \tilde{\omega} \sim 1/\tilde{R}(E),$$

which define the border of the fully coherent parton region. For  $x_\perp > \tilde{R}(E)$  the parton interaction with the target is weak and is represented by the “classical” elastic scattering and the soft classical gravitational wave emission.

## 4 Collision of two AS disks

Firstly, let us consider an interaction of two transplanckian particles, “represented” by such parton disks, in a formal way - by the regge like machinery.

<sup>11</sup>There is an interesting question, concerning the transparency of this black disk, filled with hard gravitons at a saturated density, and of the dependence of this transparency from energy. At first it seems that for the saturated parton disk, with the finite 2-dimensional density of degrees of freedom, the transparency ( $= |S(y, b)|^2$ ) should remain finite (grey disk) and not  $\rightarrow 0$  when  $E \rightarrow \infty$ . But this contradicts probably to the longitudinal boost invariance of the transparency at a given impact parameter calculated in the parton model. The same problem emerges in the QCD when we try to estimate the transparency of the saturated Froissart disk [22]. But there, with the growth of energy, more higher transverse momenta scales enter the game. And although on every such scale saturated density is finite, the total density grows with  $E$  and the disk becomes more and more black. How this question is solved for gravity is unclear.

Usually in this case one starts from a Green function corresponding to a basic Regge object (like bare pomeron) and then, using it, one can build various higher order diagrams for amplitudes and inclusive cross-sections. In our case this implies to start from 2G pole with  $\alpha(0) = 3 + \Delta$  corresponding to (23). But we make one step forward and start directly from the “economized” 2G object. For pomerons this step corresponds to a transition to “Froissarons”, which are the economized sums of pomerons, and then to construction of higher diagrams using such objects [24]. Applying this approach to our case we form the basic reggeon Green function - proportional to the amplitude corresponding to the S-matrix (31) :

$$D(y, b) = i(1 - S(y, b)) \sim i \theta(R_{\perp}^2(y) - b^2) + D^{soft}(y, b), \quad (36)$$

where  $D^{soft}(y, b)$  is the soft part of  $D$  containing gravitons with  $\omega$ ,  $k_{\perp} \ll m_p$ . Using this  $D(y, b)$  one can construct higher reggeon diagrams and various inclusive cross-sections. The hard inelastic cross section is given by

$$\sigma_{in}(Y) = \int d^2B \text{Im}D(Y, B) \simeq \pi R_{\perp}^2(Y) + \sigma_{in}^{soft}(Y) \quad (37)$$

as considered in the previous section. The corresponding inclusive cross-section for hard gravitons with the definite impact parameter  $b$  and the rapidity  $y$  and the initial  $Y$  and  $B$  is given by the reggeon diagram with two cut D s - it takes in the impact parameter representation a simple form

$$\begin{aligned} \rho(y, b, Y, B) &\simeq V \text{Im}D(y, b) \cdot \text{Im}D(Y - y, B - b) = \\ &= V \theta(R_{\perp}^2(y) - b^2) \cdot \theta(R_{\perp}^2(Y - y) - (B - b)^2) + \rho^{soft}(y, b, Y, B), \end{aligned} \quad (38)$$

where  $V$  - is the inclusive graviton emission vertex, and the  $\rho^{soft}$  - the soft contribution. Other higher inclusive cross sections can be constructed in the similar way. The region where such  $\rho(y, b, Y, B)$  is big is shown in Fig.4. The higher

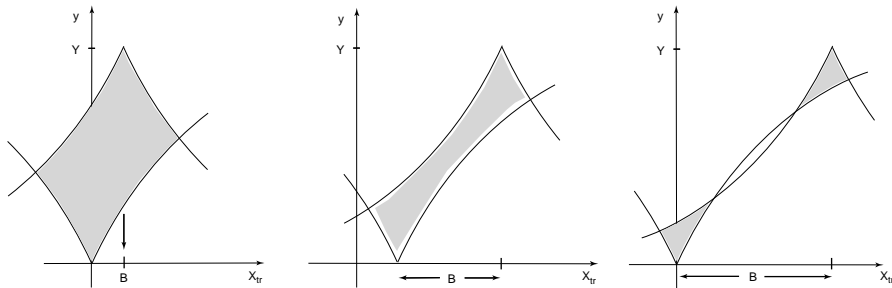


**Fig.4 :** The shape of region of intersection of black disks in  $(x_{\perp} * y)$  space at various  $B$ . The width of shaded region at given rapidity is connected with value of inclusive cross-section as represented in Fig.6

loop corrections in  $D$  do not change the structure of the inclusive cross-section in the “black” part of  $D(y, b)$  i.e. at  $b < R_{\perp}(y)$ , but can be essential at the border of the AS-disk, where their influence on a diffractive and a soft radiation processes (like in the case of Froissaron [24] ) is not a small.

Now let us try to interpret the expressions (38) in the parton language. In terms of multiparticle Fock space components this is rather a complicated task and is not yet considered in full details even for a simple scalar multiperipheral interaction. But we know many qualitative aspects of such processes from the space-time interpretation of various ladder and eikonal diagrams corresponding to a reggeon exchange. We consider separately soft and hard gravitons. Because most of partons in the AS disk have energies  $\omega \sim m_p$  we will consider firstly only them.

**Hard graviton production.**

At given rapidity  $y$  and  $\vec{x}_\perp$  hard gravitons can be produced only from a collision at the same rapidity and  $\vec{x}_\perp$  of black components of two disks. This corresponds directly to the “two  $\theta$ ” intersection term in (38). Then the full inclusive spectrum at the same  $y$  is proportional to the area of the intersection of two black parts of AS disks at the given rapidity. So, for definite  $B$  and  $y$ , we can have three different configuration of disks intersections as shown in Fig.5. In the

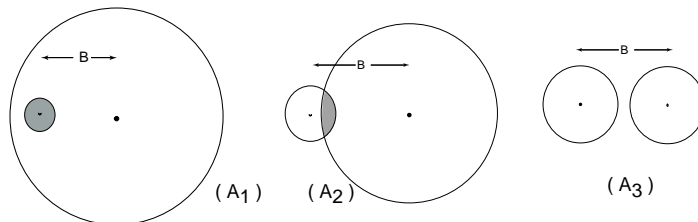


**Fig.5 :** Configuration of intersecting black AS disks is shown at three rapidities:  $A_1$  - closer to the fragmentation region,  $A_3$  - in the center of mass system. This can be compared with spectra at Fig.6 at  $B > B_{cr}$

cases ( $A_1$ ) and ( $A_2$ ) the two AS-disks intersect - and the area of the intersection, in Planck units,  $A(B, R_\perp(E_1), R_\perp(E_2))$  defines the value of hard inclusive cross-section. In the configuration (b) there is no intersection of the black parts of the disk - so the contribution to the hard inclusive cross-section at these  $B$  and  $y$  is zero. We neglect effects of smeared hard disk borders and then the hard inclusive density at given  $B$  and  $y$  is approximately given by

$$\rho(B, y, Y) \simeq m_p^2 A(B, R_1, R_2), \quad (39)$$

where  $R_1 = R_\perp(E_1)$ ,  $R_2 = R_\perp(E_2)$ ,  $E_1 = m_p e^y$ ,  $E_2 = m_p e^{Y-y}$ , and the area of the black disk intersection can be represented as

$$A \simeq \int d^2 x_\perp \theta(R_1^2 - x_\perp^2) \theta(R_2^2 - |x_\perp - B|^2) \Rightarrow \quad (40)$$

$$A = \zeta_1 R_1^2 + \zeta_2 R_2^2 \quad \text{for} \quad |R_1 - R_2| < B < R_1 + R_2 ,$$

$$A = \min(\pi R_1^2, \pi R_2^2) \quad \text{for} \quad B < |R_1 - R_2| ,$$

where

$$\zeta_1 = \theta_1 - \frac{1}{2} \sin 2\theta_1 , \quad \zeta_2 = \theta_2 - \frac{1}{2} \sin 2\theta_2 ,$$



$$\cos \theta_1 = \frac{B^2 + R_1^2 - R_2^2}{2BR_1}, \quad \cos \theta_2 = \frac{B^2 + R_2^2 - R_1^2}{2BR_2}$$

The structure of hard graviton spectra in rapidity, corresponding to (39,40), is illustrated at Fig.6 <sup>12</sup>. It changes from highly peaked in c.m.s. for  $B \sim 0$  to the purely diffractive like spectra with two filled bumps near the fragmentation region of colliding particles for large  $B \sim m_p^{-2}\sqrt{s}$ . The gap in inclusive spectra

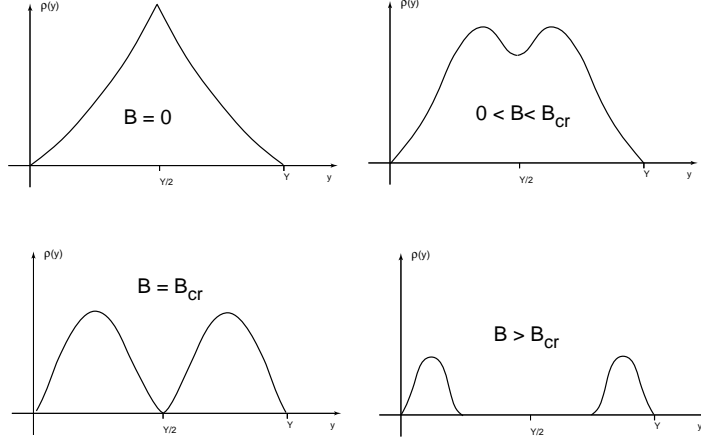


**Fig.6 :** Hard gravitons inclusive spectra in rapidity (a,b,c,d) for various values of the impact parameter  $B$ , where  $B_{cr} = 2R_{\perp}(\sqrt{s}/2)$ .

around the central position  $y = Y/2$  is formed when  $B > B_{cr}$ , where the  $B_{cr}$  correspond to a configuration when two hard disk in c.m.s. only touch each other, i.e.  $2R_{\perp}(Y/2) = B_{cr}$ . The multiplicity of produced gravitons and the maximal value of the spectra at Fig.6 also depends strongly from  $B$ , and drastically changes their behaviour at  $B \sim B_{cr} \sim m_p^{-1}(s/m_p^2)^{1/4}$ . From (40) one can simply estimate the behaviour of the mean multiplicity of hard gravitons as a function of  $s$  and  $B$ :

$$N(B, s) = \theta(B_{cr} - B) \frac{\sqrt{s}}{m_p} f\left(\frac{B}{B_{cr}(s)}\right) + \theta(B - B_{cr}) \frac{s}{m_p^4 B^2}, \quad (41)$$

where the function  $f(B/B_{cr}) = m_p s^{-1/2} \int dy A(B, R_{\perp}(y), R_{\perp}(Y - y))$  depends slowly on the argument. The multiplicity distribution due to (40) is also mainly defined by geometrical parameters of collision, and the probability to produce  $n$  hard gravitons

$$w_n \simeq \frac{1}{n^3} + \left(\frac{m_p^2}{s}\right)^{-3/2} f_1\left(n \frac{m_p}{\sqrt{s}}\right) \theta(n - n_{cr}) \quad (42)$$

is fast decreasing almost for all  $n$ . The small additional term with the slowly varying function  $f_1 \sim 1$  in r.h.s. of (42) is essential only for  $n > n_{cr} \sim \sqrt{s}/m_p$ . It comes from collisions with  $B < B_{cr}(s)$ . Although the total inelastic cross-section (37) for the production of hard gravitons is big  $\sim sm_p^{-4}$ , the corresponding

<sup>12</sup>Later on we put  $\Delta = 0$ . This simplifies expressions and at the same time corresponds probably to the correct value.

final state contains a small number of particles (Fig.6 d). The processes (Fig.6 a,b,c) , where the hard multiplicity in final state is high  $\sim \sqrt{s}$ , come only from collisions with  $B < B_{cr}$  - their cross-section is  $\sim m_p^{-3/2} \sqrt{s}$ .

The mean hard graviton multiplicity corresponding to (42) is low  $\langle n \rangle \sim 1$  at all  $s$ , and the dispersion of the multiplicity grows:  $\langle n - \langle n \rangle \rangle^2 \sim \ln s$ , but not so fast <sup>13</sup>.

Note that as a result of such behaviour of  $w_n$  the full inclusive spectra of hard gravitons integrated over  $B$  takes a very simple scaling form

$$\begin{aligned} \tilde{\rho}(y, Y) &= \sigma_{in}^{-1}(Y) \int d^2 B \rho(B, y, Y) \simeq \\ &\simeq \frac{\pi m_p^2 R_1^2 R_2^2}{R^2(s)} = \pi \frac{E_1 \cdot E_2}{m_p E} \sim const(y, Y) \sim 1 \end{aligned} \quad (43)$$

like in the case of constant asymptotic cross-sections. Although here the fluctuations in shape of the individual events can be very big and are mainly governed by the distribution of impact parameters, like in the case of a nucleus-nucleus collision.

***The role of soft gravitons and the longitudinal boost behaviour.***

We have not considered explicitly the production of low energy gravitons with  $\omega \ll m_p$  and of the soft gravitons with  $k_\perp \ll m_p$ . There are two types of such processes. In one, which takes place on large impact parameters, only the soft gravitons are produced. Such processes must be more or less satisfactorily described by the perturbative methods - and the complete space-time picture will be not far from that corresponding to a classically described gravitational wave radiation during a fast particles collision, for example like that given in [2].

The other processes, taking place at smaller  $B$ , also contains soft gravitons accompanying hard gravitons created as a result of a collision of black AS disks. But here the soft and low energy partons also enter directly in the production of hard gravitons. The consideration of their interaction is needed to consistently explain (in parton terms) the generation of hard particles for relatively big impact parameters  $B_{cr} < B < m_p^{-2} \sqrt{s}$  , and the inclusive spectra of type Fig.6d, when we view on a collision from the c.m.s., where the hard disks do not collide directly.

The related more general question concerns the invariance of cross-sections and reactions outcomes under longitudinal boost transformations. The parton state of fast particles changes under such boosts in a complicated and nontrivial way: the mean number of partons and their space configuration changes etc. Therefore the requirement of the invariance of various cross-sections calculated in the parton approach under boost, corresponds to very strong condition, essentially restricting the structure of the parton state itself <sup>14</sup>.

<sup>13</sup>This radically differs from possible expectations, when for all  $B < m_p^{-2} \sqrt{s}$  the big black hole (possibly rotating) is created, leading at the end to a almost full dissipation of the initial energy into soft in c.m.s. particles.

<sup>14</sup>In the massive theories like QCD, the rate of the growth of a parton black disk radius  $R_\perp(E)$  is almost completely fixed by the invariance of the inelastic cross-section  $\sigma_{in} = \pi(R_\perp(E_1\xi) + R_\perp(E_2/\xi))^2$  under changes of the boost parameter  $\xi$ . Such a condition leads only to two solutions :  $R_\perp(E) = const(E)$  and  $R_\perp(E) = c \ln E$ . This corresponds either to  $\sigma_{in}(E) = const$  or  $\sigma_{in}(E) \sim \ln^2 E$  - that is the Froissart-like behaviour. Moreover, by same method one can show that in the Froissart case only the black (not a gray) disk case

Let's consider the interaction of the AS disk with  $E_1 \gg m_p$  with an almost massless particle which can have a "low" energy  $E_2 \ll m_p$  - so that it can be considered as "test" objects and in the same way choose the full  $s \simeq 2E_1 E_2 \gg m_p^2$ .

Then examine the behavior of this system under the longitudinal boost - when the transformed energies become

$$E_1 \rightarrow E_1 \xi, \quad E_2 \rightarrow E_2/\xi, \quad (44)$$

but the impact parameters  $B$  and  $s$  are not changed.

Firstly choose  $B = B_1 < R_\perp(s) \sim m_p^{-1}(s/m_p^2)^{1/4}$  so that the hard gravitons are produced in the final state. If  $\xi$  are such that  $E_2 \sim m_p$  then we have the collision of the  $AS_1$  black disk with a hard particle, which is inelastically scattered by a disk with the probability = 1. After that the production of secondary hard gravitons starts almost immediately and the real particles appear at times  $\sim m_p^{-1}$ . Call this frame - frame I and fix  $\xi \sim 1$  in this frame.

If we choose next  $\xi$  such that  $E_2 \ll m_p$  then we must suppose that the interaction of the " $E_2$ " particle with the hard saturated  $AS_1$  disk at the same  $B$  takes place with the same probability = 1, although the cross-section of the interaction with individual partons decreased  $\sim 1/\xi^2$ . Now the  $AS_1$  parton system is only "softly" excited during the interaction. After that the instabilities in the  $AS_1$  disk grow gradually and first hard gravitons will be created only after the AS disk moves in  $z$  on  $\sim m_p^{-1} \xi$  from the collision place. Let's call this frame - frame II.

But for such  $\xi$  (in frame II) the radius of the black part of the  $AS_1$  disk, where partons are in the saturated phase, is also increased

$$R_\perp(E_1) \rightarrow R_\perp(E_1 \xi) = \xi^{1/2} R_\perp(E_1).$$

Therefore the " $E_2$ " particle should be absorbed by a disk with the probability = 1 for larger  $B$  up to  $\xi^{1/2} R_\perp(E_1)$ . This probability of the particle " $E_2$ " interact at  $B = B_2$  where  $R_\perp(E_1) < B_2 < R_\perp(E_1 \xi)$  must not depend on  $\xi$ . In the frame I at  $B = B_2$  the " $E_2$ " particle does not collide directly with a black disk. Now directly with the black disk can interact only soft partons accompanying the particle " $E_2$ ". And this mechanism can regulate the boost invariance of the probability interaction = 1. This role of soft partons-gravitons is even more evident if, at the same  $B = B_2$ , we select  $\xi$  so to move to c.m. system, where the black disks are most far one from another in the transverse direction.

One can estimate simply maximal impact parameters for which the capture of soft partons from one colliding particle by the black disk of another particle take place with the probability = 1. For the capture of soft partons we need to choose  $B$  and  $\omega$  so that as minimum as one soft parton from " $AS_2$ " falls into the black disk of  $AS_1$  or vice versa - this gives :

$$\hat{n}(E_2, \omega, B) \cdot R_\perp^2(E_1, \omega_1 \sim m_p) \sim m_p^{-2}$$

From the other hand, the size of the transverse localization of the soft parton, which is  $\sim 1/\omega$ , must be much less than the  $AS_1$  black disk radius  $R_\perp(E_1, \omega_1 \sim$  is allowed. The other restriction can also be found by the same way. The reason why the bust invariance of cross-sections is so restrictive for parton states is probably connected with that it plays the role of t-unitarity which is very essential for high energy amplitudes, but can not be explicitly imposed on parton wave functions [22].

$m_p$ ). Otherwise the soft parton will mainly elastically scatter on the black disk and not be captured by him. This corresponds to the condition for minimal  $\omega$  :

$$\omega \cdot R_{\perp}(E_1, m_p) \sim 1$$

Then, using expressions (33),(35) for  $\hat{n}$  and  $R_{\perp}$ , it is simple to find  $B = R_{\perp max}$  and  $\omega$  fulfilling these two conditions in the case of the arbitrary intercept  $\Delta$  :

$$\omega_{min} \sim m_p \left( \frac{m_p}{E_1} \right)^{(2+\Delta)/4}, \quad (Bm_p)^2 \sim \left( \frac{E_1}{m_p} \right)^{1+\frac{3}{4}\Delta+\frac{1}{8}\Delta^2} \left( \frac{E_2}{m_p} \right)^{1+\Delta/2}$$

The inelastic processes up to such big impact parameters  $B \sim R_{\perp max}$  are essentially influenced by “strong” gravity mechanisms. The corresponding hard inelastic cross-section

$$\sigma_{in}(E_1, E_2) \sim (R_{\perp max})^2 \sim m_p^{-2} \left( \frac{E_1}{m_p} \right)^{1+\frac{3}{4}\Delta+\frac{1}{8}\Delta^2} \left( \frac{E_2}{m_p} \right)^{1+\Delta/2} \quad (45)$$

can be boost invariant under (44) only if the powers of  $E_1$  and  $E_2$  in (45) are equal - because only in this case  $2E_1E_2 \sim s$  does not depend on  $\xi$ . This gives condition on  $\Delta$  with two solutions

$$\Delta = 0, \quad \Delta = -2$$

The first solution corresponds to the hard  $\sigma_{in} \sim sm_p^{-4}$  cross-section which we have discussed above and gives the additional arguments for the  $\Delta = 0$  case. The second solution corresponds (a little peculiarly) to asymptotically constant cross-sections, typical for hadron interactions and associated with a pomeron.

## 5 Instability of the final state. The black holes creation after collision

Before the collision, in parton black disks of incoming particles, we already have too much ‘low’ energy transverse partons-gravitons so that in fact the full virtual energy is concentrated in them. But this state is evidently stable under the implosive collapse due to strong phase correlations between these partons. During the collision some partons are exited and “disrelated”, and later become free with the inclusive spectra of type (38). Only after that the possible long-range gravitational instabilities in the evolved particles system can lead to the formation of various density clusters over the “initially smooth”  $\rho(y)$  background.

The main attractive instability can take place for groups of created particles having close longitudinal velocities. We can divide conditionally the  $\rho(y)$  spectrum in layers in the rapidity of the width  $\delta \sim 1$  in such a way that the relative energies of particles(gravitons) from the same layer are not high, and the hard partons from the neighbor layers look ultrarelativistic. In a first moment the created particles density in every such layer is high - close to the critical. Therefore these particles (gravitons) strongly interact one with another during some period of time before there density becomes so small that they can move almost free. During this period of time the relative energies of particles in layer are partially thermalized and they behave in fact as a massive particles. It is

essential that because of such multipole scattering on “media”, for some period of time particles can not escape from layer as free massless particles. In fact such condition fixes the value of  $\delta$  and the portion of particles that are “confined” in layer.

If we go to a longitudinal system with a definite rapidity  $y_1$ , where some layer is “standing” (marked in Fig.7) then we see that particles from other layers move fast away. In fact in the corresponding time scale these particles can be still in the virtual state and become free only after time  $t \sim \exp|y - y_1|$ . So we can consider this layer separately from the others. Its mass is

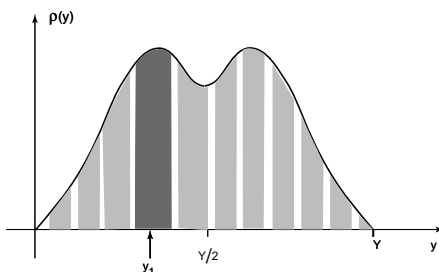


**Fig.7 :** Inclusive spectra for hard gravitons divided on layers in rapidity. These layers can transform during the following evolution into black holes with the same rapidities and masses  $\sim \rho(y)$ .

$$M(y_1) \sim m_p^3 A(y_1, Y, B) \sim \rho(y_1, Y, B) , \quad (46)$$

where  $A$  is the transverse area of the “ $y_1$ ” layer. This mass is concentrated in the region of the space with the longitudinal size  $\sim m_p^{-1} \exp(\delta)$  and the transverse size  $\sim \sqrt{A}$ . These magnitudes are much less than the size of the horizon of the BH with the same mass  $M(y_1)$ , and at the same time particles constituting this mass are not ultrarelativistic. Therefore the most part of particles from such a layer at time  $\sim \sqrt{A}$  transforms in a black hole with the mass  $M(y_1)$  and the transverse position, defined by the center of the region  $A$ . During this time the horizon “surrounding” these particles transforms from a pancake-like configuration to sphere.

The neighbours to “ $y_1$ ” layers “ $y_1 - \delta$ ” and “ $y_1 + \delta$ ” also transform to black holes with masses  $m_p \rho(y_1 - \delta)$  and  $m_p \rho(y_1 + \delta)$ , but this will take place later and they will have the relative to “ $y_1$ ” velocities  $\sim 1$ . So gradually the chain of black holes will be produced whose distribution in longitudinal momenta is typically multiperipheral and close to the uniform<sup>15</sup> - with  $\rho = \text{const}(y) \sim \delta^{-1}$ . But their masses are different at fixed  $B$  and are given by values of  $\rho(y_1, Y, B)$ . On average - when we integrate over  $B$  then the mean masses of produced BH are also constant over  $y$  and small  $\sim m_p$ , because the main contribution comes from the large  $B$ .

Because every such BH is produced from a layer of partons having approximately the same longitudinal rapidity, these BH will be non-rotating. This is accurate within the small “thermal” fluctuation, and border effects. Because the borders of layers are slightly asymmetric for  $B \neq 0$  (see Fig.4) some angular

<sup>15</sup>In fact uniform distribution in rapidity can be slightly distorted, because the effective widths of layers in rapidity can be correlated with there masses.

momentum can be concentrated there. The main part of the angular momentum from the initial state (especially for large  $B$ ) is transferred to the relative motion of the created BH and to the surrounding particles not captured by BH.

The rapidity distribution of produced BH in the individual events is controlled mainly by the corresponding values of  $B$  and repeats the curves in Fig.6. For  $B < B_c = m_p^{-1}(E/m_p)^{1/4}$  we have a continuous (multiperipheral) in  $y$  chain of BH, whose masses are given by curves Fig.6(a-b). For  $B > B_c$  two chains of black holes moving in forward and backward directions are created - their masses repeat again the behaviour of  $\rho(y, Y, B)$  in Fig.6(c,d). These chains are separated by the rapidity gap of width  $\Delta y \simeq Y - 2 \ln(Bm_p)$  and for big  $\Delta y$  when  $B \sim \sqrt{s}/m_p^2$  correspond to a typical diffractive generation of black holes<sup>16</sup>.

Probably the part of particles falling between layers can escape and not captured by one of BH. Their percentage is possibly not big, but it is complicated to estimate them by the qualitative methods used here.

It remains a question : can some of these black holes (or all of them) merge during the future evolution, if the rate of longitudinal grow of there horizons is faster than these BS separate one from another. In fact this is a purely classical GR problem, and it needs additional investigation. Here we present only following qualitative argument.

The longitudinal structure of particles system created in a collision of black AS disks is similar to the one-dimensional homogeneous expanding cosmological solution. In both cases particles are “injected” initially in such a way that in every longitudinally boosted frame we locally see particles flying away with the same 2D density and the momentum distribution. Usually for such expanding system the small long-range density perturbations are damped with time or not growth. Only a short-range (scale  $\delta$ ) large density fluctuations, created on the initial “viscous” stage, can growth and clusterize. But on a scale much larger than this no new structures emerge.

## 6 Conclusion and the final remarks

Thus we come to a picture of gravitational interactions at  $E \gg m_p$  which is in some respect reminiscent to the picture of asymptotic hadronic (QCD) interactions in the Froissart limit: the transplanckian particles collision looks like an interaction of black disks with the production of particles in the geometrical intersection region of disks. The essential difference is that for the gravitational

---

<sup>16</sup> Above we discussed how complicated can be the “trajectories” leading from the colliding particles state to a final state containing the BH. Such trajectories are evidently absent in the semiclassical probability estimate  $\exp(-S_{gr}(\tilde{g}))$ , when we put in Euclidean classical action  $S_{gr}$  some continued solutions  $\tilde{g}$  containing the BH. There are two ways to cure this. In one, we must put all higher radiative correction in the Euclidean action (the necessary number grows with the energy). Then the corresponding equation of motion can have necessary trajectories  $\tilde{g}$  with a low value of effective action and a high statistical weight. The other way is to use the classical action and consider the transition to the BH not from the few particle initial state, but from the specially prepared multiparticle state (parton component), containing approximately the same number of degrees of freedom as the entropy of the BH. But in both cases the “advantages” of the Euclidean approach disappear and the consideration in the Minkowski frame is much simpler. This is in fact the general reason because the Euclidean methods do not work properly at high energies.

interaction the radiuses of these black disks grow much faster  $\sim E^{1/2}$  with energy, as compared to the QCD case, where these radiuses grow relatively slow  $\sim \ln E$ . The other distinction is the character of the interaction in the final state. In the QCD the final state hadronization is short-range and so this does not essentially change the structure of the final state. But for the gravitational case we have a long-range attractive interaction which can create a “multiperipheral” chain of black holes. Finally all this difference is the consequence of the masslessness of gravitons. If QCD were massless at large distances then probably also there can some similar phenomena originate - like powerlike growth with energy of inelastic cross-sections, etc.

Additional remarks in conclusion.

- At “not too high” energies  $s \sim m_p^2$ , when both black disks from hard partons are only in the embryonic state, it is complicated to make any quantitative conclusion (in particular - predict the threshold for the first BH creation and their mass) by the methods we used. Here all essential parameters are of order of unity and the possible dynamics can be rather involved. But there are also no reasons to expect that the purely classical estimates give reliable values.
- This model can probably extended to the case with additional hidden dimensions  $D > 4$ . Here one can distinguish two cases
  - a) “Small” additional compact dimensions, with the radius close to the Planck scale  $\sim m_p$ . In this case all higher Kalusa-Klein modes act simply as massive particles strongly coupled at the scale  $\sim m_p$  to gravitons. Probably they do not change any qualitative aspect of picture, but contribute “only” to various renormalization of numerical parameters.
  - b) If the size of additional dimensions (or of some of them) in which gravitons can penetrate is very large compared to the 4 D Planck scale, as in the case of the TeV gravity [17], then some aspects of the picture can change more essentially. In this case too much depends on the concrete realization of the gravity in the brane world. For example, in the case of only large and non warped additional dimensions we simply have the  $D > 4$ dim. gravity, but some particles (and the colliding ones also) are glued to 3 space dimensions. Then we have the transverse graviton spectrum  $dn \sim (E^2 d\omega/\omega^3) d^{D-2}(k_\perp/m_p)$ . This leads to a black D-2 dimensional disk filled with partons at the Planck density with the radius

$$R(E) \sim m_p^{-1} \left( E/m_p \right)^{1/(D-2)}$$

and to cross-sections  $\sigma_{in} \sim R^2(E)$ . By the same way one can find the created hard graviton density  $\rho(y, B, Y \sim m_p^{D-2} A((B, y, Y))$ , where  $A$  is now the  $D - 2$  dim. volume of the colliding disk intersection region. Qualitatively the B dependence on  $\rho$  is the same as in Fig.6. In the final state one can again expect the gravitational long-range instability and the produced particles clusterization into the chain of black holes. But now (and here much depends on the details of brane world models) created gravitons and black holes can move in large additional dimensions and dissipate there. In corresponding “accelerator events” this can look out

as if a part of the colliding energy escapes. Evidently there can be many variations of this simple scenario.

- In this model the elastic scattering amplitude contains components coming from different sources. One is Coulomb like - it comes from the “classical” soft graviton exchange at large impact parameters. Of same type are the soft long-range multiperipheral corrections. The other one corresponds to the imaginary diffraction contribution to the elastic amplitude generated by the big inelastic cross-section  $\sim m_p^{-2}(s/m_p^2)$ .

The finite angle high energy elastic scattering usually comes from small impact parameters and is triggered by the fluctuations in which in an initial state one has only few (minimally possible) number of partons, concentrated in a small size volume. For transplanckian collisions this corresponds at least to components of partonic wave functions of both particles without hard black disks. This probability is  $\sim \exp(-s/m_p^2 C)$ , and this leads to the too fast decreasing term in the finite angle scattering cross-section :

$$d\sigma/d\theta \sim \frac{s}{m_p^4} \exp\left(-\frac{s}{m_p^2}C(\theta)\right) + \left(d\sigma/d\theta\right)_{soft},$$

where  $\left(d\sigma/d\theta\right)_{soft} \sim \exp(-c_1\sqrt{s})$  is the large impact parameter contribution, generated by the multiple scattering. This behaviour can be compared with the Cerulus-Martin bound and with the finite angle cross-section for a string scattering [25].

## ACKNOWLEDGMENTS

I would like to thank A.B. Kaidalov and K.A. Ter-Martirosyan for useful conversations and comments and I.N. Kancheli for help and advices.

A financial support of RFBR through the grants 01-02-17383 and 00-15-96786 is gratefully acknowledged. This work was also supported by the INTAS grant 00-00366 and NATO grant PSTCLG 977275 .

## References

- [1] P.D. D’Eath, *Phys. Rev.* **D 18**, (1977) 990.
- [2] P.D. D’Eath and P.N. Payne, *Phys. Rev.* **D 46**,(1992) 658.
- [3] L.N. Lipatov, *Phys.Lett*, **116B** (1982) 411.
- [4] L.N. Lipatov, *Nucl. Phys.* **B365**, (1991) 614.
- [5] I.J. Muzinich and M. Soldate, *Phys. Rev.* **D37** (1988) 359.
- [6] D. Amati, M. Ciafaloni and G. Veneziano, *Phys. Lett.* **B197** (1987) 81.
- [7] D. Amati, M. Ciafaloni and G. Veneciano, *Phys.Lett*, **B 289** (1992) 87.
- [8] D. Amati, M. Ciafaloni and G. Veneciano, *Nucl. Phys.* **B347** (1990) 550.



- [9] G. 't Hooft, *Phys.Lett*, **B 198** (1987) 61.
- [10] T. Banks and W. Fischler, arXiv:hep-th/9906038.
- [11] S.B. Giddings, arXiv:hep-ph/0110127.
- [12] G.F. Giudice, R. Rattazzi and J.D. Wells, arXiv:hep-th/0112161.
- [13] S. Dimopoulos and G. Landsberg, arXiv:hep-ph/0106295.
- [14] M.V. Voloshin, arXiv:hep-ph/0107119 , 0111099.
- [15] S.B. Giddings and S. Thomas, arXiv:hep-ph/0106219.
- [16] D.M.Eardley and S.B. Giddings, arXiv:gr-qc/0201034.
- [17] N. Arkani-Hamed, S. Dimopoulos and G. Dvali, *Phys.Lett* **B429** (1998) 263.
- [18] P.S. Aichelburg and R.U. Sexl, *Gen.Rel Grav.* 2 (1971)303.
- [19] J.J. Atick and E. Witten, *Nucl. Phys.* **B310** (1988) 291.
- [20] C.B. Thorn, arXiv:hep-th/9405069, arXiv:hep-th/9607204.
- [21] L. Susskind *Phys. Rev. D* **54**,5463 (1996).
- [22] O.V. Kancheli, arXiv:hep-ph/0106219.
- [23] E.A.Kuraev and L.N.Lipatov,V.S.Fadin, *Sov.Phys.JETP* **44** (1976) 443.
- [24] J.L. Cardy *Nucl.Phys.* **B 75** (1974) 413.
- [25] D.F.Gross and P.F.Mende, *Phys.Lett* **B197** (1987) 129.